Role of ligand substitution on long range electron transfer in azurins

Farver, O.; Jeuken, L.J.C.; Canters, G.W.; Pecht, I.

Eur. J. Biochem. **267**, 3123–3129 (2000) © FEBS 2000

Role of ligand substitution on long-range electron transfer in azurins

Ole Farver,[1] Lars J. C. Jeuken,[2] Gerard W. Canters[2] and Israel Pecht[3]

[1]*Institute of Analytical and Pharmaceutical Chemistry, The Royal Danish School of Pharmacy, Copenhagen, Denmark;* [2]*Leiden Institute of Chemistry, Leiden University, Gorlaeus Laboratories, Leiden, The Netherlands;* [3]*Department of Immunology, The Weizmann Institute of Science, Rehovot, Israel*

Azurin contains two potential redox sites, a copper centre and, at the opposite end of the molecule, a cystine disulfide (RSSR). Intramolecular electron transfer between a pulse radiolytically produced $RSSR^-$ radical anion and the blue Cu(II) ion was studied in a series of azurins in which single-site mutations were introduced into the copper ligand sphere. In the Met121His mutant, the rate constant for intramolecular electron transfer is half that of the corresponding wild-type azurin. In the His46Gly and His117Gly mutants, a water molecule is co-ordinated to the copper ion when no external ligands are added. Both these mutants also exhibit slower intramolecular electron transfer than the corresponding wild-type azurin. However, for the His117Gly mutant in the presence of excess imidazole, an azurin–imidazole complex is formed and the intramolecular electron-transfer rate increases considerably, becoming threefold faster than that observed in the native protein. Activation parameters for all these electron-transfer processes were determined and combined with data from earlier studies on intramolecular electron transfer in wild-type and single-site-mutated azurins. A linear relationship between activation enthalpy and activation entropy was observed. These results are discussed in terms of reorganization energies, driving force and possible electron-transfer pathways.

Keywords: azurin; electron transfer; enthalpy–entropy compensation; Marcus theory; pulse radiolysis.

Electron transfer plays an important role in many biological systems, and a central question is to what extent do specific structural properties of proteins affect the rates of electron transfer [1–6]. The blue single-copper protein, azurin, which serves as an electron mediator in certain bacteria, has become an effective model for the study of intramolecular long-range electron transfer (LRET) in proteins [7–12]. The 3D structures have been determined for a large number of wild-type and single-site-mutated azurins [13–18] and shown to consist of a rigid β-sheeted polypeptide. As it contains two potential redox centres, i.e. the copper ion co-ordinated directly to amino acid residues and a disulfide bridge (RSSR) at opposite ends of the barrel-shaped molecule, no additional external redox group is required to study internal LRET. Indeed, we have previously demonstrated that LRET between these two centres can be induced by pulse-radiolytic single-electron reduction of RSSR [7–12].

We have examined the effect of specific structural changes on the rate of intramolecular electron transfer between the $RSSR^-$ radical and the Cu(II) centre in both wild-type and single-site-mutated azurins. In the present study, we used a series of azurin mutants in which modifications were introduced into the copper ligand sphere. Two mutants (His46Gly and His117Gly) contain a free co-ordination site. In the absence of external ligands, water will bind at the copper site [19]. Alternatively, in the presence of excess imidazole, the latter may take up the vacant position at the copper centre [20,21]. In another mutant (Met121His), the weakly co-ordinating Met121 was substituted with a more strongly binding histidine [18,22]. The internal LRET in these mutants was studied in order to (a) examine the effect of copper ligand substitutions on the electron transfer rates and (b) try to resolve two previously determined potential pathways leading to the Cu(II) centre via two different ligands. To analyse the role of the polypeptide matrix separating donor (D) and acceptor (A), we used the structure-dependent pathway model developed by Beratan & Onuchic for identifying potential electron-transfer routes [23,24].

Correspondence to O. Farver, Institute of Analytical and Pharmaceutical Chemistry, The Royal Danish School of Pharmacy, 2 Universitetsparken, DK-2100 Copenhagen, Denmark. Fax: + 45 3530 6013, Tel.: + 45 3530 6269, E-mail: of@dfh.dk

Abbreviation: LRET, long-range electron transfer.

(Received 10 January 2000; accepted 16 March 2000)

MATERIALS AND METHODS

Proteins

Wild-type azurins of *Pseudomonas aeruginosa* [25] and *Alcaligenes denitrificans* [26], *Ps. aeruginosa* His117Gly azurin [26], *A. denitrificans* His46Gly azurin [21] and *A. denitrificans* Met121His azurin [22] were isolated as described previously. His117Gly and His46Gly azurin were isolated in their apo forms and reconstituted shortly before the experiments by adding 1 equiv. $Cu(NO_3)_2$ to N_2O-saturated protein solutions. After the addition of copper, His46Gly azurin was used immediately whereas His117Gly azurin was incubated for 20–30 min at room temperature. When imidazole was introduced to replace water as an additional ligand, it was added to His117Gly azurin to a final concentration of 0.5 mM after the incubation with $Cu(NO_3)_2$ and left to equilibrate for at least another 10 min. A_{280} was used to determine the concentration of the apo form of His46Gly and His117Gly azurin ($\varepsilon_{280} = 9.1\ mM^{-1}\cdot cm^{-1}$).

Aqueous solutions, 0.1 M in sodium formate and 10 mM in phosphate (pH 4.0), were deaerated and saturated with N_2O by continuously bubbling in glass syringes. For the experiments on His46Gly azurin, formate concentrations were decreased to

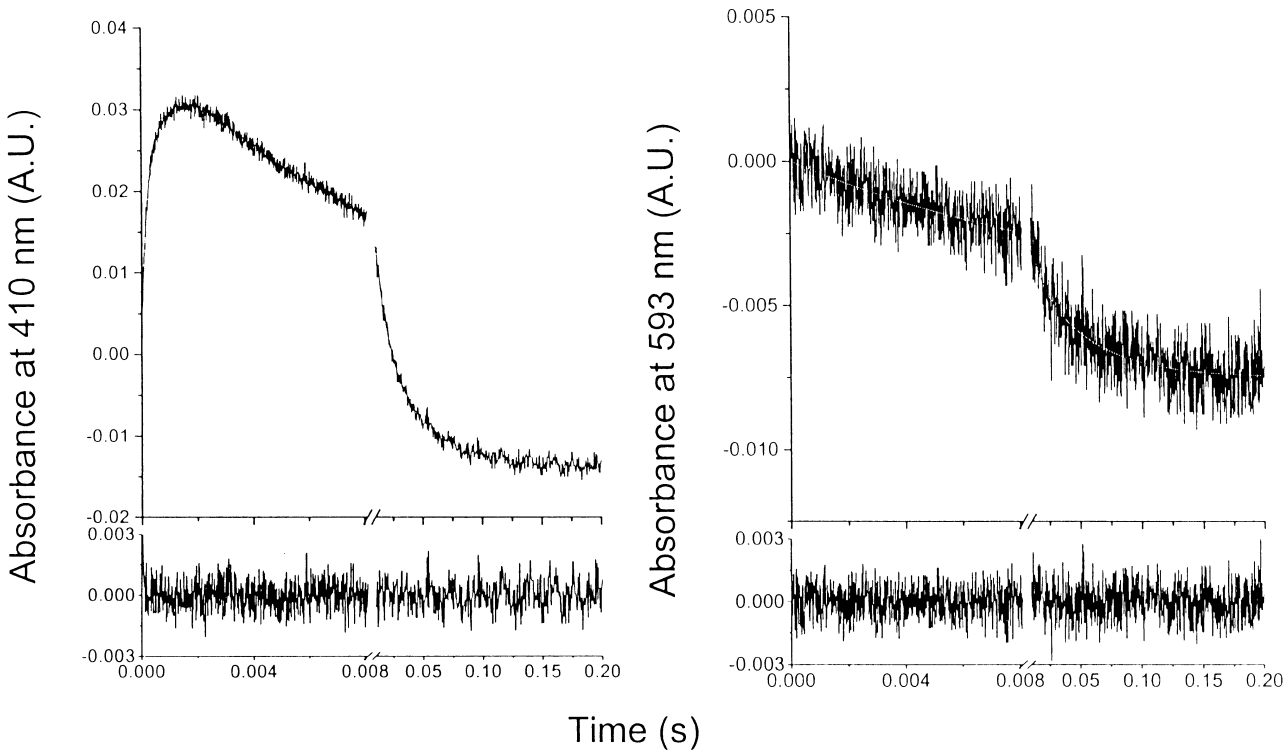

Fig. 1. Time-resolved spectra of the Met121His azurin mutant. The protein concentration was 10 μM in an N_2O-saturated solution containing 100 mM formate and 5 mM phosphate, pH 7.0. Temperature 26.1 °C; Pulse width 0.5 μs; optical path length 12.3 cm. Left: 410 nm, monitoring formation and decay of the $RSSR^-$ radical anion. Right: 593 nm, monitoring reduction of Cu(II) in two phases.

10 mM to minimize formate ligation to the copper ion. A dissociation constant of 0.25 M was determined for the formate complex with His46Gly azurin [21]. Thus, under the above conditions, formate binding was negligible.

After pH adjustment to 7.0 by titration with 0.5 or 0.05 M NaOH, the concentrated protein stock solution was added. N_2O bubbling was continued for another 5 min, and the solution was then transferred anaerobically to the pulse-radiolysis cuvette.

Kinetic measurements

Pulse-radiolysis experiments were carried out using the Varian V-7715 linear accelerator at the Hebrew University in Jerusalem. Electrons accelerated to 5 MeV were employed, using pulse lengths in the range 0.1–1.5 μs, equivalent to 0.6–10 μM CO_2^- radical ions. All optical measurements were carried out anaerobically, under purified argon at a pressure slightly in excess of 1 atm in a 4 × 2 × 1 cm Spectrosil cuvette. Three light passes were employed, which resulted in an overall optical path length of 12.3 cm. A 150-W xenon lamp produced the analysing light beam, and appropriate optical filters with cut-off at 385 nm were used to avoid photochemistry and light scattering. The data-acquisition system consisted of a Tektronix 390 A/D transient recorder and a PC. In each experiment, 2000 data points were collected, divided equally between two different time scales. Usually the processes were followed over at least three half-lives. Each kinetic run was repeated at least four times. The data were fitted to a sum of exponentials using a non-linear least-squares program written in MATLAB®. The temperature of the reaction solutions was controlled and continuously monitored by a thermocouple attached to the cuvette. Almost all reactions were performed under pseudo-first-order conditions, with typically a 10-fold excess of oxidized protein over reductant. All chemicals were of analytical grade and used without further purification. Milli-Q water was used throughout the studies.

RESULTS

Pulse-radiolytically produced CO_2^- radicals reduce both redox-active sites of the azurins, the copper site and the disulfide bridge, at essentially diffusion-controlled rates [7–12]. In wild-type azurins the Cu(II) → Cu(I) reduction results in an absorption decrease around 600 nm whereas the $RSSR^-$ radicals that are formed absorb at 410 nm. These two bimolecular reactions are depicted below (Reactions i and ii). After this fast phase, the $RSSR^-$ transient was found to decay (Reaction iii) concomitantly with a further decrease in the characteristic Cu(II) absorption (the slow phase).

$$RSSR\text{–}Az[Cu(II)] + CO_2^- \rightarrow RSSR\text{–}Az[Cu(I)] + CO_2 \quad \text{(i)}$$

$$RSSR\text{–}Az[Cu(II)] + CO_2^- \rightarrow RSSR^-\text{–}Az[Cu(II)] + CO_2 \quad \text{(ii)}$$

$$RSSR^-\text{–}Az[Cu(II)] \rightarrow RSSR\text{–}Az[Cu(I)] \quad \text{(iii)}$$

A. denitrificans wild-type azurin and its Met121His mutant

A. denitrificans Met121His azurin exhibits two intense Cu(II) absorption bands (at 439 and 593 nm), rather than the one observed in wild-type azurin. Hence, the absorption changes following the pulses are slightly different from those of the wild-type: at 593 nm a decrease in absorption is still observed in the fast phase, due to direct bimolecular Cu(II) reduction by CO_2^- (Reaction i). In the fast phase monitored at 410 nm, however, because of overlap of the Cu(II) and $RSSR^-$

Table 1. Kinetic and thermodynamic data for intramolecular reduction of Cu(II) by $RSSR^-$ at 298 K and pH 7.0.

Azurin	k_{298} (s^{-1})	$E^{\circ'}$ (mV)	$-\Delta G^{\circ}$ [a] ($kJ \cdot mol^{-1}$)	$\Delta H^{\neq}$ ($kJ \cdot mol^{-1}$)	$\Delta S^{\neq}$ ($J \cdot K^{-1} \cdot mol^{-1}$)
Ps. aeruginosa [b]	44 ± 7	304 ± 5	68.9 ± 2.3	47.5 ± 2.2	−56.5 ± 3.5
H46G·*aq*	15 ± 2	< 300 [c]	< 68.5	42.1 ± 3.5	−81 ± 5
H117G·*aq*	7 ± 3	< 300 [c]	< 68.5	22.0 ± 3.2	−155 ± 11
H117G·*im*	149 ± 17	240 ± 20 [d]	62.7 ± 6.5	54.5 ± 3.9	−22 ± 1
A. denitrificans	42 ± 4	305 ± 5	69.0 ± 2.3	43.5 ± 2.5	−67 ± 9
M121H	21 ± 4	215 ± 5[e]	60.3 ± 2.8	28.0 ± 2.1	−127 ± 8

[a] Calculated from the measured Cu(II)/Cu(I) electrode potentials and assuming $E^{\circ'} = -410 \pm 5$ mV for the $RSSR/RSSR^-$ couple in all the azurins studied here. [b] Taken from [11]. [c] Estimates based on the data in [27]. [d] Taken from [27]. [e] Taken from [22].

absorption bands, the changes depend on the oxidation state of the protein, and either a decrease or an increase in absorbance is observed (Reactions i and ii). When the $RSSR^-$ anion is produced in [Cu(II)]Az, electron transfer to Cu(II) is observed in the slower phase (Reaction iii). This reaction is seen in both wild-type and Met121His azurin as a concomitant absorption decrease at 410 and around 600 nm. As oxidized Met121His azurin also absorbs at 410 nm, the time-dependent spectrum at this wavelength ends below the initial baseline (Fig. 1).

Electron transfer may occur either intramolecularly (Reaction iii) in the above reaction scheme, or between two protein molecules. To distinguish between these two possibilities, the concentration dependencies of the observed rates of $RSSR^- \rightarrow$ Cu(II) electron transfer were determined, typically in the range 1–10 μM oxidized azurin. The observed rate constants for *A. denitrificans* wild-type azurin exhibited a slight concentration dependence at protein concentrations above ≈ 5 μM, indicating a small contribution from intermolecular electron transfer, and from this dependence the intramolecular rate constant was extracted. Similar intermolecular electron transfer has also been observed in other azurins [11]. At pH 7.0 and 298 K, the rate constant for intramolecular electron transfer in *A. denitrificans* wild-type azurin is 42 ± 4 s^{-1} (Table 1). The electron-transfer rate constant for Met121His azurin was independent of protein concentration between 1 and 10 μM and is half that of wild-type azurin, i.e. 21 ± 4 s^{-1}. The activation parameters for both proteins were determined by measuring electron-transfer rates as a function of temperature (Table 1). The lower rate constant of Met121His azurin is due to a more negative activation entropy, although this is partly compensated for by a decrease in activation enthalpy (Table 1).

Ps. aeruginosa His46Gly and His117Gly azurin mutants

Experiments were performed on *Ps. aeruginosa* His117Gly azurin in the presence and absence of imidazole. However, studies on the His46Gly azurin were only carried out in the absence of imidazole or any other external ligands. Because of the high dissociation constant of the oxidized His46Gly azurin–imidazole complex (2.7 mM) [21] compared with 24 μM for oxidized H117G azurin–imidazole (L. J. C. Jeuken, P. van Vliet, R. C. Acosta, J. McEvoy, F. A. Armstrong & G. W. Canters, unpublished results), experiments using the imidazole complex of His46Gly azurin were not feasible for practical reasons.

The reaction pattern observed for the His117Gly azurin–imidazole complex (His117Gly·*im*) was similar to that of wild-type *Ps. aeruginosa* azurin (*vide supra*). The intramolecular electron-transfer rate constant was determined to be 149 ± 17 s^{-1} at 25 °C, which is threefold higher than for wild-type azurin (Table 1). As the activation parameters determined for this process show, this higher rate is mostly due to a smaller (negative) activation entropy (Table 1).

The observed absorption changes in the *Ps. aeruginosa* His117Gly azurin aqua form (His117Gly·*aq*) are similar to those of *A. denitrificans* Met121His azurin, in as much as the Cu(II) centres of both mutants exhibit considerable absorption at 410 nm. However, a difference was resolved between the electron-transfer rate constants determined at 410 nm and 628 nm in *Ps. aeruginosa* His117Gly·*aq* the first wavelength giving higher values at temperatures above 15 °C. As rate constants for intramolecular electron transfer in this mutant are one order of magnitude smaller than in wild-type *Ps. aeruginosa* azurin, a competing $RSSR^-$ dismutation reaction is probably observed at 410 nm. Therefore, the parameters presented in Table 1 are based on data obtained at 628 nm only.

His46Gly·*aq* also exhibits slow intramolecular electron transfer. Because the Cu(II) centre in this azurin mutant shows relatively weak absorption at 630 nm, reduction could not be monitored independently of that of the decay of the $RSSR^-$ anion band at 410 nm. However, at temperatures above 15 °C, two separate exponential processes could be resolved in the kinetic traces recorded at 410 nm. As the slower decay process was also observed in samples in which the copper ion has already been reduced, it was excluded from being due to internal LRET from $RSSR^-$ to Cu(II). Therefore the parameters were derived from the fast decay phase only (20 °C and higher) and are presented in Table 1. As for His117Gly·*aq*, the electron-transfer rate constant is lower than in wild-type azurin, because both mutants exhibit a more negative activation entropy. However, in the case of His117Gly·*aq*, part of this effect is counteracted by a lower activation enthalpy.

DISCUSSION

The semiclassical Marcus theory for non-adiabatic intramolecular electron transfer predicts that rates are governed by the standard free energy of reaction (ΔG^0), the nuclear reorganization energy (λ), the distance separating electron donor (D) and acceptor (A), and the electronic coupling (H_{DA}) of D and A at the transition state [28]:

$$k = \frac{2\pi}{\hbar} \cdot \frac{H_{DA}^2}{\sqrt{(4\pi\lambda RT)}} e^{-(\Delta G^0 + \lambda)^2 / 4\lambda RT} \quad (1)$$

The electronic coupling energy, H_{DA}, is expected to decay exponentially with the distance separating D and A as:

$$H_{DA} = H_{DA}^0 e^{-\frac{\beta}{2}(r - r_0)} \quad (2)$$

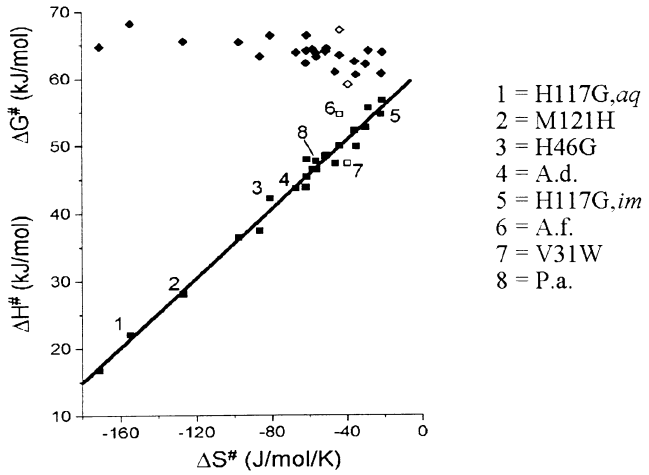

Fig. 2. Activation enthalpy (squares) and activation free energy, calculated at $T = 298$ K (diamonds), as a function of the entropy of activation for a series of azurins taken from the literature. 1, H117G·*aq*; 2, M121H; 3, H46G; 4, *A. denitrificans* wild-type; 5, H117G·*im*; 6, *A. faecalis* wild-type; 7, V31W; 8, *Ps. aeruginosa* wild-type. The points numbered 1–5 and 8 refer to the present work. The straight line represents the linear least-squares fit to the data points ('compensation line'). The open symbols represent the systems with the largest deviations from the compensation line.

When the distance between A and D is considerable (1.0 nm), only very limited electronic coupling will exist. However, intramolecular electron-transfer reactions proceeding over distances of 2.0 nm or more have been observed [29].

In order to understand the variation in electron-transfer rates more clearly, we determined the activation enthalpy and entropy further (Table 1). The activation enthalpy is given by the following relation [28]:

$$\Delta H^{\neq} = \frac{\lambda}{4} + \frac{\Delta H^0}{2}\left(1 + \frac{\Delta G^0}{\lambda}\right) - \frac{(\Delta G^0)^2}{4\lambda} \qquad (3)$$

The entropy of activation includes a contribution from the distance dependence of the electronic coupling [28] (cf. Eqn 2):

$$\Delta S^{\neq} = \Delta S^* - R\beta(r - r_0) \qquad (4)$$

where β is the electronic coupling decay factor. ΔS^* is related to the standard entropy change, ΔS^0 [28]:

$$\Delta S^* = \tfrac{1}{2}\Delta S^0(1 + \Delta G^0/\lambda) \qquad (5)$$

For wild-type *Ps. aeruginosa* azurin $\beta(r - r_0)$ has been determined to be 24.6 for the LRET from the S-S bridge to Cu(II) [11].

For a series of reactions of similar type, the phenomenon of a linear relationship between enthalpy and entropy of activation is well documented [30,31]. In Fig. 2 the activation enthalpy is plotted against the activation entropy for a range of wild-type and single-site-mutated azurins. The relationship is linear with a slope of $T_C = 258 \pm 6$ K and a correlation coefficient of 0.99. Such enthalpy–entropy compensation is commonly found for closely related reactions, with observed slopes in the 250–315 K range for reactions in aqueous solution [31,32]. Hypotheses explaining enthalpy–entropy compensation include changes in solvent reorganization, particularly in hydrogen-bonding solvents [31,32]. While linear behavior may be related to the properties of water, deviation of the linear relationship of a certain data point is explained by a diverging property of that typical reaction. As a consequence of the fact that the compensation temperature, T_C, is close to the experimental temperature range, the observed free energy of activation, $\Delta G^{\neq}$, at 298 K is nearly invariable (63 ± 4 kJ·mol^{-1}) over the full range of reactions, although there is a small systematic decrease in $\Delta G^{\neq}$ with decreasing $\Delta S^{\neq}$ (Fig. 2), amounting to a small but systematic increase in the electron-transfer rate.

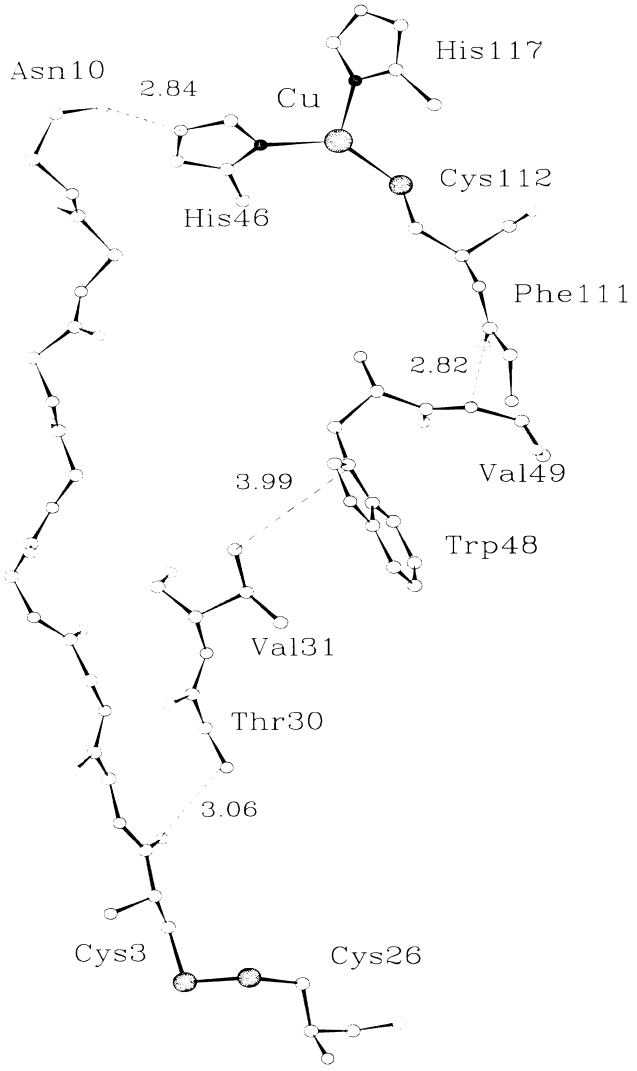

Fig. 3. Calculated electron-transfer pathways from the sulfur of Cys3 to the copper ligands Cys112 and His46. Some interconnecting distances (in Å) are shown.

Pathway calculations

Pathway calculations by the Beratan & Onuchic algorithm [23,24] for intramolecular electron transfer were performed using the high-resolution 3D structures of *Ps. aeruginosa* and *A. denitrificans* azurins and those available for their mutants [13–17]. In this algorithm, the overall electronic coupling of a pathway is calculated as a product of the couplings of the constitutive individual links. The optimal electronic coupling between the two redox sites is then identified. For all the azurins examined so far, the calculations predict similar electron-transfer routes [10,11] (Fig. 3): one, longer path, proceeds through the peptide chain from Cys3 of the disulfide bridge to the copper-ligating imidazole of His46; and a second, shorter path, that also starts from Cys3 but proceeds through the

indole ring of Trp48 to the copper ligating thiolate of Cys112. For these two routes, the electronic coupling decay factors were found to be $\Pi\varepsilon = 2.5 \times 10^{-7}$ and 3.0×10^{-8}, respectively [11]. However, in these calculations the electronic interactions between the Cu(II) ion and its ligands were not included. As a high degree of anisotropic covalency has been shown to exist in the blue single-copper protein, plastocyanin, electron transfer through the Cys ligand would be markedly enhanced [33,34]. By similar arguments, from Ψ_{HOMO} ligand coefficients in azurin calculated by Larsson *et al*. [35], it can be estimated that the rate of electron transfer through the Cys112 ligand would also be enhanced by a factor of ≈ 150 over electron transfer via one of the His ligands. The pathway calculations combined with the notion of anisotropic covalency would therefore suggest that the 'Trp48' pathway would be more advantageous than the one proceeding through His46.

By modifying the copper binding site, the charge distribution on Cu and the co-ordination sphere will certainly change. An effect of the electron delocalization on the electronic coupling between donor and acceptor will appear as an apparent change in the activation entropy (Eqn 4). From the observed changes in the EPR hyperfine splitting (A_z) of the different mutants, we have obtained information on the degree of electronic delocalization for the three mutants, Met121His, His46 Gly and His117Gly. A decrease in electronic density on the cysteine would give rise to a larger hyperfine splitting (A_z) [36].

A. denitrificans Met121His azurin

While spectroscopic and structural studies have revealed the simultaneous existence of multiple conformations of *A. denitrificans* Met121His azurin [37], at neutral pH a species with a tetrahedral copper site was found to be the dominant one, where His121 co-ordinates directly to the copper ion with a Cu–$N^{\delta 1}$ bond distance of 2.22 Å. This is in contrast with the Cu–S^{δ} (Met121) distance of 3.11 Å in wild-type azurin [15]. Spectroscopic studies show that the novel structure of *A. denitrificans* Met121His azurin modulates the electronic character of the Cu(II) ion, creating a so-called 'Type 1.5' site at neutral pH [22]. Instead of the normal single intense absorption band around 600 nm observed for blue copper proteins, this mutant exhibits two strong absorption bands at 439 and 593 nm. Like the 593 nm transition, the band at 439 nm results from a ligand to metal charge-transfer transition. In native blue copper proteins, the intensity of this band is usually low [38,39]. The EPR spectra show an increase in hyperfine splitting (A_z) from 0.0062 cm^{-1} in wild-type *A. denitrificans* azurin [40] to 0.0102 cm^{-1} in Met121His azurin [22], suggesting a lower delocalization of the unpaired electron [36]. This may reduce the rate of electron transfer via Cys112, although the point corresponding to Met121His in Fig. 2 lies close to the correlation line and, in this respect, seems to behave normally. The *A. denitrificans* Met121His electron-transfer kinetics should be compared with those of wild-type *A. denitrificans* azurin, as the mutation was applied to this wild-type protein. The smaller electron-transfer rate constant of this mutant is connected to the position of the Met121His point in Fig. 2 downwards along the correlation line.

Ps. aeruginosa His46Gly and His117Gly azurins

The experiments using a mutant in which His46 is replaced by Gly were aimed at probing the relevance of the 'His46' pathway relative to the Trp48 route, as this would be blocked when the linkage to the copper ion via the hydrogen bond from Asn10 to His46 is lost. However, this mutation also considerably modifies the co-ordination sphere of the copper ion [21], and this may also affect the electron-transfer rate. Therefore, to investigate the effect of the change in electronic properties caused by removal of a His ligand and its effect on the electron-transfer rate, the kinetics of electron transfer in a similar mutant, *Ps. aeruginosa* His117Gly azurin, were also studied. The Cu(II) ion in both His46Gly and His117Gly mutants of *Ps. aeruginosa* was found to be accessible to external ligands which, on co-ordination to the metal ion, obviously change its spectroscopic features [20,21,41]. For example, in the absence of other ligands, a water molecule is co-ordinated to the copper ion [19] and His117Gly·*aq* exhibits intense optical absorption bands at 420 nm and 628 nm, which give rise to its green color. His46Gly·*aq* exhibits similar bands at 400 and 630 nm, although the 630-nm absorption is very low and cannot be used to monitor the copper oxidation state. The hyperfine splitting (A_z) in His117Gly·*aq* is 0.0139 cm^{-1} [20] whereas in His46Gly·*aq* it is 0.0160 cm^{-1} [21]. This should be compared with the corresponding coupling in wild-type *Ps. aeruginosa* azurin (0.0058 cm^{-1}) [40]. As for Met121His azurin, the higher value of the hyperfine splitting suggests a lower delocalization of the unpaired electron. This may influence the electron coupling of the electron-transfer reaction, which would appear as an apparent change in the activation entropy (Eqn 4). Indeed, the higher hyperfine splittings (A_z) in the EPR spectra of the three mutants correspond to more negative activation entropies.

The data summarized in Fig. 2 show that the points for His46Gly·*aq* (no. 3) and His117Gly·*aq* (no. 1) as well as for wild-type *Ps. aeruginosa* (no. 8) all lie very close to the correlation line. This implies that the same mechanism of electron transfer is operating in all three proteins [30–32], indicating that the dominating pathway for LRET in azurin is the 'Trp48' route from Cys3 to the Cys112 copper ligand.

The relevance of the 'Trp48' route is confirmed by the two data sets that deviate most from the linear relationship between the activation entropy and enthalpy (Fig. 2), which are for wild-type *A. faecalis* azurin (no. 6) and *Ps. aeruginosa* Val31Trp azurin (no. 7). Val31 is part of the 'Trp48' electron-tunnelling pathway from the disulfide bridge to the copper site (Fig. 3). Wild-type azurin from *A. faecalis* is unusual among azurins in that it lacks Val at position 31 which is occupied by an Ile residue. It also has a Val at position 48 instead of a Trp.

When sufficient imidazole is added to solutions of *Ps. aeruginosa* His46Gly or *Ps. aeruginosa* His117Gly, co-ordination to the copper ion occurs, and the mutants turn blue, with main absorption bands at 628 nm (His117Gly·*im*) and 621 nm (His46Gly·*im*), which is close to that of wild-type azurin (626 nm) [20,21]. Other spectroscopic features, such as EPR, ENDOR and resonance Raman spectra, are also restored [20,21,42,43]. This implies that the structures of the mutants and the geometry of their metal site are maintained despite the replacement of the histidine by imidazole.

The rate constant of intramolecular electron transfer in His117Gly·*im* is considerably faster than in wild-type *Ps. aeruginosa* azurin in spite of the lower driving force (Table 1). As their activation enthalpies are comparable, within experimental error, the reorganization energy is probably not changed significantly (Eqn 3). Figure 2 demonstrates that, in spite of the large difference in electron-transfer rates, the points for His117Gly·*aq* (no. 1 on Fig. 2), His46Gly·*aq* (no. 3 on Fig. 2), His117Gly·*im* (no. 5 on Fig. 2) and wild-type *Ps. aeruginosa* azurin (no. 8 on Fig. 2) fit perfectly on the $\Delta H^{\#}$ vs. $\Delta S^{\#}$ compensation plot. In His46Gly·*aq* and His117Gly·*aq*, water molecules can enter the copper co-ordination sphere and give

rise to rather large changes in the solvation sphere. Inserting an imidazole, however, which fits perfectly in the pocket of H117G azurin, will to a certain extent prevent water from approaching the redox site. Nevertheless, all three data points extending the full range of the plot (Fig. 2) lie on the straight line as expected, indicating operation of one and the same electron-transfer mechanism.

Conclusion

Evidently, single-site mutations at the metal co-ordination site produce multiple changes in electron-transfer reactivity and essentially affect all four main parameters that govern LRET: driving force, reorganization energy, and in some cases also the separation distance and nature of the protein matrix. In spite of the complexity of interpreting the results of the present study, the Trp48 electron-transfer pathway seems to be favored over the His46 pathway.

ACKNOWLEDGEMENTS

This research was supported by the Danish Natural Science Research Council, the Volkswagen Foundation, the German–Israeli Foundation, and the Dutch Ministries of Economic Affairs, of Education, Culture and Science, and of Agriculture, Nature Management and Fishery in the framework of an industrial research program of the Association of Biotechnological Research Schools in the Netherlands (ABON).

REFERENCES

1. Beratan, D.N., Onuchic, J.N., Winkler, J.R. & Gray, H.B. (1992) Electron-tunneling pathways in proteins. *Science* **258**, 1740–1741.
2. Broo, A. & Larsson, S. (1992) Electron-transfer in azurin and the role of aromatic side groups of the protein. *J. Phys. Chem.* **95**, 4925–4928.
3. Farid, R.S., Moser, C.C. & Dutton, P.L. (1993) Electron-transfer in proteins. *Curr. Opin. Struct. Biol.* **3**, 225–233.
4. Gray, H.B. & Winkler, J.R. (1996) Electron transfer in proteins. *Annu. Rev. Biochem.* **65**, 537–561.
5. Moser, C.C., Keske, J.M., Warncke, K., Farid, R.S. & Dutton, P.L. (1992) Nature of biological electron-transfer. *Nature (London)* **355**, 796–802.
6. Siddarth, P. & Marcus, R.A. (1993) Correlation between theory and experiment in electron-transfer reactions in protein: electronic couplings in modified cytochrome-*c* and myoglobin derivatives. *J. Phys. Chem.* **97**, 13078–13082.
7. Farver, O. & Pecht, I. (1989) Long-range intramolecualr electron-transfer in azurins. *Proc. Natl Acad. Sci. USA* **86**, 6968–6972.
8. Farver, O. & Pecht, I. (1992) Long-range intramolecular electron-transfer in azurins. *J. Am. Chem. Soc.* **114**, 5764–5767.
9. Farver, O., Skov, L.K., van de Kamp, M., Canters, G.W. & Pecht, I. (1992) The effect of driving force on intramolecular electron-transfer in proteins – studies on single-site mutated azurins. *Eur. J. Biochem.* **210**, 399–403.
10. Farver, O., Skov, L.K., Pascher, T., Karlsson, B.G., Nordling, M., Lundberg, L.G., Vanngard, T. & Pecht, I. (1993) Intramolecular electron-transfer in single-site-mutated azurins. *Biochemistry* **32**, 7317–7322.
11. Farver, O., Skov, L.K., Gilardi, G., van Pouderoyen, G., Canters, G.W., Wherland, S. & Pecht, I. (1996) Structure-function correlation of intramolecular electron transfer in wild type and single-site mutated azurins. *Chem. Phys.* **204**, 271–277.
12. Farver, O., Bonander, N., Skov, L.K. & Pecht, I. (1996) The pH dependence of intramolecular electron transfer in azurins. *Inorg. Chim. Acta* **243**, 127–133.
13. Baker, E.N. (1988) Structure of azurin from Alcaligenes denitrificans refinement at 1.8 Å resolution and comparison of the two crystallographically independent molecules. *J. Mol. Biol.* **203**, 1071–1095.
14. Hammann, C., Messerschmidt, A., Huber, R., Nar, H., Gilardi, G. & Canters, G.W. (1996) X-ray crystal structure of the two site-specific mutants Ile7Ser and Phe110Ser of azurin from *Pseudomonas aeruginosa*. *J. Mol. Biol.* **255**, 362–366.
15. Nar, H., Messerschmidt, A., Huber, R., van de Kamp, M. & Canters, G.W. (1991) Crystal structure analysis of oxidized Pseudomonas aeruginosa azurin at pH 5.5 and pH 9.0. A pH-induced conformational transition involves a peptide bond flip. *J. Mol. Biol.* **221**, 765–772.
16. Nar, H., Messerschmidt, A., Huber, R., van de Kamp, M. & Canters, G.W. (1991) X-ray crystal structure of the two site-specific mutants His35Gln and His35Leu of azurin from *Pseudomonas aeruginosa*. *J. Mol. Biol.* **218**, 427–447.
17. Romero, A., Hoitink, C.W., Nar, H., Huber, R., Messerschmidt, A. & Canters, G.W. (1993) X-ray analysis and spectroscopic characterization of M121Q azurin. A copper site model for stellacyanin. *J. Mol. Biol.* **229**, 1007–1021.
18. Messerschmidt, A., Prade, L., Kroes, S.J., Sanders-Loehr, J., Huber, R. & Canters, G.W. (1998) Rack-induced metal binding vs. flexibility: Met121His azurin crystal structures at different pH. *Proc. Natl Acad. Sci. USA* **95**, 3443–3448.
19. Kroes, S.J., Salgado, J., Parigi, G., Luchinat, C. & Canters, G.W. (1996) Electron relaxation and solvent accessibility of the metal site in wild-type and mutated azurins as determined from nuclear magnetic relaxation dispersion experiments. *J. Biol. Inorg. Chem.* **1**, 551–559.
20. den Blaauwen, T. & Canters, G.W. (1993) Creation of type 1 and type 2 copper site by addition of exogenous ligands to the *Pseudomonas aeruginosa* azurin His117Gly mutant. *J. Am. Chem. Soc.* **115**, 1121–1129.
21. van Pouderoyen, G., Andrew, C.R., Loehr, T.M., Sanders-Loehr, J., Mazumdar, S., Allen, H., Hill, H.A.O. & Canters, G.W. (1996) Spectroscopic and mechanistic studies of type-1 and type-2 copper sites in Pseudomonas aeruginosa azurin as obtained by addition of external ligands to mutant His46Gly. *Biochemistry* **35**, 1397–1407.
22. Kroes, S.J., Hoitink, C.G., Andrew, C.R., Ai, J.Y., Sanders-Loehr, J., Messerschmidt, A., Hagen, W.R. & Canters, G.W. (1996) The mutation Met121 → His creates a type-1.5 copper site in Alcaligenes denitrificans azurin. *Eur. J. Biochem.* **240**, 342–351.
23. Regan, J.J., Risser, S.M., Beratan, D.N. & Onuchic, J.N. (1993) Protein electron-transport – single versus multiple pathways. *J. Phys. Chem.* **97**, 13083–13088.
24. Skourtis, S.S., Regan, J.J. & Onuchic, J.N. (1994) Electron-transfer in proteins: a novel-approach for the description of donor-accaptor coupling. *J. Phys. Chem.* **98**, 3379–3388.
25. van de Kamp, M., Hali, F.C., Rosato, N., Agro, A.F. & Canters, G.W. (1990) Purification and characterization of a non-reconstitutable azurin, obtained by heterologous expression of the *Pseudomonas aeruginosa* azu gene in *Escherichia coli*. *Biochim. Biophys. Acta* **1019**, 283–292.
26. den Blaauwen, T., van de Kamp, M. & Canters, G.W. (1991) Type I and type II copper sites obtained by external addition of ligands to a His117Gly azurin mutant. *J. Am. Chem. Soc.* **113**, 5050–5052.
27. Reference withdrawn.
28. Marcus, R.A. & Sutin, N. (1985) Electron transfer in chemistry and biology. *Biochim. Biophys. Acta* **811**, 265–322.
29. Clarke, M.J., Goodenough, J.B., Jorgensen, C.K., Neilands, J.B., Reinen, D. & Weiss, R., eds. (1991) *Structure and Bonding: Long Range Electron Transfer in Biology.* Springer-Verlag, Berlin and Heidelberg.
30. Wherland, S. & Gray, H.B. (1977) Electron transfer mechanisms employed by metalloproteins. In *Biological Aspects of Inorganic Chemistry* (Dolphin, D., ed.), pp. 289–368. J. Wiley, New York.
31. Grunwald, E. & Steel, C. (1995) Solvent reorganisation and thermodynamic enthalpy–entropy compensation. *J. Am. Chem. Soc.* **117**, 5687–5692.
32. Leffler, J.E. (1955) The enthalpy–entropy relationship and its implications for organic chemistry. *J. Org. Chem.* **20**, 1202–1231.
33. Christensen, H.E.M., Conrad, L.S., Mikkelsen, K.V., Nielsen, M.K. & Ulstrup, J. (1990) Direct and superexchange electron-tunneling at

the adjectent and remote sites of higher-plant plastocyanins. *Inorg. Chem.* **29**, 2808–2816.

34. Lowery, M.D., Guckert, J.A., Gebhard, M.S. & Solomon, E.I. (1993) Active-site electronic-structure contributions to electron-transfer pathways in rubredoxin and plastocyanin: direct versus super-exchange. *J. Am. Chem. Soc.* **115**, 3012–3013.
35. Larsson, S., Broo, A. & Sjolin, L. (1995) Connection between structure, electronic-spectrum, and electron-transfer properties of blue copper proteins. *J. Phys. Chem.* **99**, 4860–4865.
36. Shadle, S.E., Penner-Hahn, J.E., Schugar, J.H., Hedman, B., Hodgson, K.O. & Solomon, E.I. (1993) X-ray absorption spectroscopy studies of the blue copper site: metal and ligand K-edge studies to probe the origen of the epr hyperfine splitting in plastocyanin. *J. Am. Chem. Soc.* **115**, 767–776.
37. Salgado, J., Kroes, S.J., Berg, A., Moratal, J.M. & Canters, G.W. (1998) The dynamic properties of the M121H azurin metal site as studied by NMR of the paramagnetic Cu(II) and Co(II) metallo-derivatives. *J. Biol. Chem.* **273**, 177–185.
38. LaCroix, L.B., Shadle, S.E., Wang, Y.N., Averill, B.A., Hedman, B., Hodgson, K.O. & Solomon, E.I. (1996) Electronic structure of the perturbed blue copper site in nitrite reductase: spectroscopic properties, bonding, and implications for the entatic/rack state. *J. Am. Chem. Soc.* **118**, 7755–7768.
39. Pierloot, K., de Kerpel, J.O.A., Ryde, U., Olsson, M.H.M. & Roos, B.O. (1998) Relation between the structure and spectroscopic properties of blue copper proteins. *J. Am. Chem. Soc.* **120**, 13156–13166.
40. Groeneveld, C.M., Aasa, R., Reinhammar, B. & Canters, G.W. (1987) EPR of azurins from *Pseudomonas aeruginosa* and *Alcaligenes denitrificans* demonstrates pH-dependence of the copper-site geometry in *Pseudomonas aeruginosa* protein. *J. Inorg. Biochem.* **31**, 143–154.
41. den Blaauwen, T., Hoitink, C.W., Canters, G.W., Han, J., Loehr, T.M. & Sanders-Loehr, J. (1993) Resonance Raman spectroscopy of the azurin His117Gly mutant. Interconversion of type 1 and type 2 copper sites through exogenous ligands. *Biochemistry* **32**, 12455–12464.
42. Coremans, J.W.A., van Gastel, M., Poluektov, O.G., Groenen, E.J.J., den Blaauwen, T., van Pouderoyen, G., Canters, G.W., Nar, H., Hammann, C. & Messerschmidt, A. (1995) An ENDOR and ESEEM study of the blue copper protein azurin. *Chem. Phys. Lett.* **235**, 202–210.
43. van Gastel, M., Coremans, J.W.A., Jeuken, L.J.C., Canters, G.W. & Groenen, E.J.J. (1998) Electron spin-echo envelope modulation spectrum of azurin at X-band. *J. Phys. Chem. A* **102**, 4462–4470.